

## HEAT TRANSFER LIMIT DUE TO PRESSURE DROP OF A LOOP THERMOSYPHON

Milanez F. H., Mantelli M. B.H.□

Mechanical Engineering Dept., Federal University of Santa Catarina  
Florianopolis, SC, Brazil, 88040-900  
Phone: +55 48 3721 9937, Fax: +55 48 3721 7615  
milanez@labtucal.ufsc.br, marcia@emc.ufsc.br

### ABSTRACT

This work presents theoretical and experimental studies on the heat transfer limit due to pressure drop of loop thermosyphons. This limit is reached when the condensate return level reaches the end of the condenser. Any further increase in the heat transfer rate makes the condensate to block part of the condenser, increasing the overall thermal resistance. No references were found on this subject in the literature. A model based on literature models and correlations for pressure drop in single and two-phase flow is developed here to predict the heat transfer limit due to pressure drop. A loop thermosyphon prototype was built and tested. The obtained data is relatively well predicted by the proposed model, showing that it can be used as a design tool for loop thermosyphons.

**KEY WORDS:** Loop Thermosyphon, Pressure Drop, Two-phase Flow

### 1. INTRODUCTION

Loop thermosyphon heat exchangers, also known as separated heat pipes, have been successfully applied in industrial waste heat recovery systems. Figure 2 presents a schematic drawing of a typical loop thermosyphon heat exchanger. Both the evaporator and the condenser are geometrically very similar. They consist of two horizontal headers (upper and lower) connected by several vertical tubes in parallel. The vapor line coming from the evaporator is connected to the upper header. As vapor condenses, the liquid flows by gravity to the lower header, which is connected back to the evaporator.

Petrobras, the Brazilian Petroleum Company, employs several large asphalt storage tanks in their plants with a capacity of more than a thousand tons. In order to keep the asphalt at the required temperature level of 140°C, the tanks are equipped with steam coils placed at the bottom. The steam is available from a 10 bar boiler that is responsible for all the steam used inside the Plant. As the boiler is located far from the tanks, large heat losses are present.

A loop thermosyphon is being developed for application in asphalt tanks heating. The objective of the thermosyphon is to replace the actual heating system. The condenser of the loop thermosyphon is

the existing steam coil. The evaporator is similar to the one shown in Fig. 1 and is placed nearby the tank and will be heated by natural gas combustion.

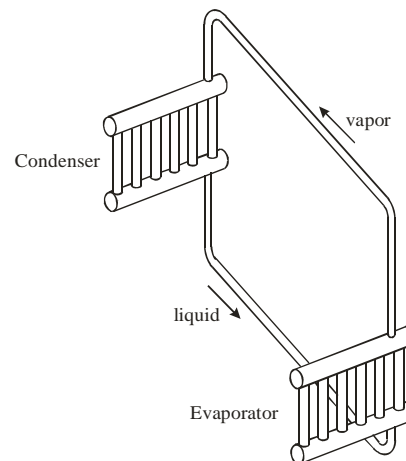


Figure 1. Separated thermosyphon heat exchanger.

Figure 2 presents a schematic of the thermosyphon under study. The main concern about this concept lies on the condenser geometry, i.e., a steam coil like. Almost the entire length of the condenser is in the horizontal orientation, apart from the “U” turns, which are slightly tilted towards the condensate flow direction. The total length of the condenser reaches hundreds on meters, which leads to considerable pressure drops to the working fluid flow.

The flow of working fluid inside a loop thermosyphon is associated to a pressure drop. The larger is the heat transfer rate through the loop thermosyphon, the larger is the working fluid velocity and the larger is the pressure drop. The pressure drop due to the working fluid flow must be compensated by a hydraulic head between evaporator and condenser. Figure 2 presents a schematic of this phenomenon. The hydraulic head  $h$  is the difference between the liquid levels in the evaporator and in the condensate return line. The maximum allowable difference is  $h_{max}$ , i.e., the vertical distance between evaporator liquid pool surface and condenser bottom. When the thermosyphon is at the heat transfer limit due to pressure drop,  $h=h_{max}$ . Any further increase in the heat transfer rate makes the condensate to block part of the condenser. A further increase in the heat transfer rate leads to  $h>h_{max}$  (see Fig. 3). The thermosyphon thermal resistance increases because the available area for two-phase heat transfer increases. That is because only the portion of the condenser that can be reached by the vapor is effective for heat transfer. The portion of the condenser that is filled with condensate no longer operates in two-phase heat transfer mode.

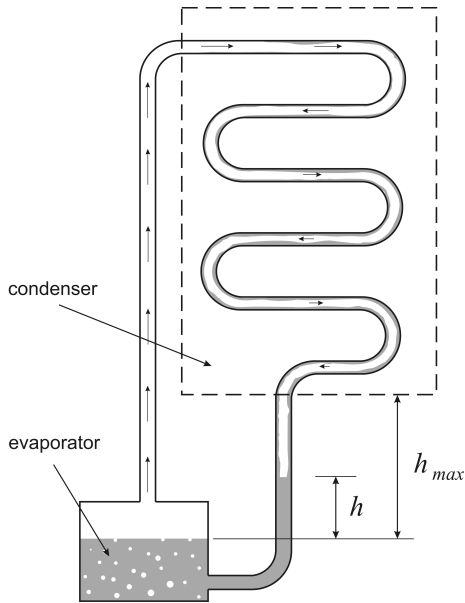


Figure 2. Hydraulic head  $h$  in a loop thermosyphon

This work presents both theoretical and experimental studies on the heat transfer limit of loop-thermosyphons. The main objective is to develop a model to help the design of loop thermosyphons.

Under normal operation, the thermosyphon should operate in the condition shown in Fig.3, i.e., below the heat transfer limit due to pressure drop.

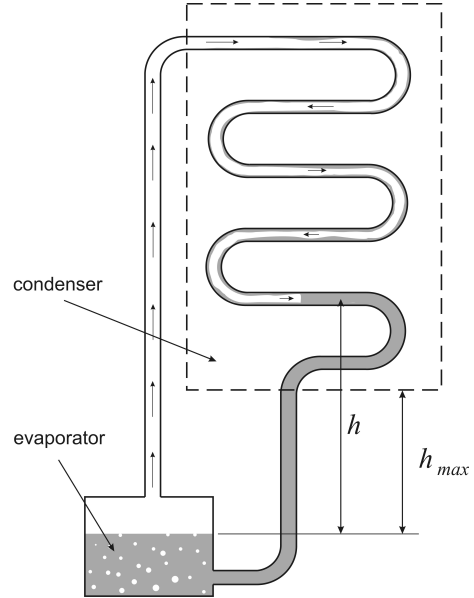


Figure 3. Loop thermosyphon beyond the pressure drop limit

## 2. THEORETICAL ANALYSIS

When the hydraulic head due to working fluid flow pressure drop is equal to the vertical distance between the liquid pool level at the evaporator and the bottom of the condenser, the loop thermosyphon is reaching a heat transfer limit. In this work, this limit is called here “the heat transfer limit due to pressure drop”. Any increase in the heat transfer rate makes the condensate level to fill up the condenser, blocking heat transfer and leading to the system’s failure. A theoretical model to predict the heat transfer limit due to pressure drop is developed here. The model is based on literature correlations and models for viscous fluid flow pressure drop.

The total pressure drop  $\Delta P_t$  of the working fluid flow is related to the hydraulic head  $h$  through the following expression:

$$\Delta P_t = (\rho_l - \rho_v) g h \quad (1)$$

where  $g=9,81 \text{ m/s}^2$ . In this equation, the pressure gradient resulting from momentum variation at the liquid-vapor interfaces were neglected.

The total pressure drop  $\Delta P_t$  is the summation of the

pressure drops due to fluid flow at the evaporator  $\Delta P_{evap}$ , vapor line  $\Delta P_v$ , condenser  $\Delta P_{cond}$  and condensate return line  $\Delta P_l$ , i.e.:

$$\Delta P_t = \Delta P_{evap} + \Delta P_v + \Delta P_{cond} + \Delta P_l \quad (2)$$

If the vapor line is well insulated so there is no condensation, the flow is single-phase (vapor). When the thermosyphon is operating at the limit, the condensate return line is filled with liquid ( $h=h_{max}$ ), and the flow in the condensate return line is also single-phase. The single-phase flow pressure drop can be calculated from classical fluid flow textbooks (Fox & McDonald, 1988), such as:

$$\Delta P = f \frac{L_e}{d_i} \frac{\rho V^2}{2} \quad (3)$$

For smooth pipes, the friction coefficient can be computed as:

$$f = \frac{0.316}{Re^{0.25}} \quad (4)$$

where Re, the Reynolds number is defined as:

$$Re \equiv \frac{\rho V D}{\mu} = \frac{4 q}{h_{lv} \pi d_i \mu} \quad (5)$$

The equivalent length  $L_e$ , appearing in Eq. (3) is the summation of the vapor line total length and the equivalent length of the bends, valves and other components of the circuit. The other two components of the pressure drop in Eq. (3), in the evaporator and in the condenser, are more complex due to the two-phase nature of the flow.

The pressure drop in two-phase fluid flow has been the subject of several researches [2,3,4]. Two classical models have been developed: homogeneous model and separated model. In the homogenous model, the two phases flow at the same velocity. In the separated model, there is a non-zero relative velocity (shear) between the phases. The results of two models are presented in the following sections. More details are provided in the references.

## 2.1 Homogeneous model

In the development of the homogeneous model for two-phase flow pressure drop it is assumed that the flow is one-dimensional and the liquid and vapor velocities are the same. In other words, the two phases are replaced by a hypothetical fluid with homogenous properties throughout all the points of

the flow. According to Collier & Thome (1994), the pressure gradient is calculated as:

$$-\frac{dP}{dz} = \frac{\left\{ \frac{2f_{TP}G^2}{\rho_l d_i} \left[ 1 + x \left( \frac{v_{lv}}{v_l} \right) \right] + \frac{g \sin \Omega}{(v_l + x v_{lv})} + G^2 v_{lv} \frac{dx}{dz} \right\}}{\left( 1 + G^2 x \frac{dv_v}{dP} \right)} \quad (6)$$

where:

$$G = \frac{\dot{m}}{A} \quad (7)$$

$$\dot{m} = \frac{q}{h_{lv}} \quad (8)$$

$$x = \frac{\dot{m}_v}{\dot{m}} \quad (9)$$

$$f_{TP} = 0,079 \left( \frac{G d_i}{\bar{\mu}} \right)^{-0,25} \quad (10)$$

The literature presents several definition for the equivalent viscosity  $\bar{\mu}$ . In this work, two models found in Wallis (1969) are used:

$$\bar{\mu} = x \mu_v + (1-x) \mu_l \quad (\text{Cicchitti}) \quad (11)$$

$$\frac{1}{\bar{\mu}} = \frac{x}{\mu_v} + \frac{(1-x)}{\mu_l} \quad (\text{McAdams}) \quad (12)$$

The second term in the denominator of Eq. (6) is related to the vapor compressibility and is normally neglected, so the denominator is approximately one. For the geometry of Fig. 3, the quality  $x$  [ ] is one at the condenser inlet and zero at the exit. Between the two points, the variation is assumed to be linear because the heat flux, and consequently the condensation rate, is uniform along the condenser length, i.e.:

$$x = 1 - \frac{z}{L_{cond}} \quad (13)$$

The condenser pressure drop is finally computed as:

$$\Delta P_{cond} = \int_0^{L_{cond}} \frac{dP}{dz} dz \quad (14)$$

where  $L_{cond}$  [m] is the total condenser length, including the equivalent lengths of the "U" bends. In this work, the equivalent length of one "U" turn is assumed to be 50 times the internal diameter of the

tube. This value was encountered in Fox & McDonnald (1988) for single-phase flow. Despite this is two-phase flow, the above value was used because of the lack of specific values.

The set of equations above are solved numerically to obtain the total pressure drop of the condenser. The condenser total length, including the equivalent length of the “U” bends, is divided in 100 parts. The pressure drop of each part is calculated considering constant values of the quantities given by Eqs. (6) and (10) to (13) within each part.

## 2.2 Separated model

As already mentioned, in the separated model, the two phases flow at different speeds. According to Collier and Thome (1994), the expression for the local pressure gradient is:

$$-\frac{dP}{dz} = \frac{1}{\Lambda} \left\{ \phi_l^2 \left[ \frac{2f_l G^2 (1-x)^2}{\rho_l d_i} \right] + [(1-\alpha)\rho_l + \alpha\rho_v] g \sin\Omega + G^2 \frac{dx}{dz} \left\{ \left[ \frac{2x}{\rho_v \alpha} - \frac{2(1-x)}{\rho_v (1-\alpha)} \right] + \frac{d\alpha}{dx} \left[ \frac{(1-x)^2}{\rho_v (1-\alpha)^2} - \frac{x^2}{\rho_l \alpha^2} \right] \right\} \right\} \quad (15)$$

where  $\Lambda \approx 1$ , which means the vapor compressibility and can be neglected (Carey, 1992), similarly to the homogeneous model. The liquid friction coefficient is calculated in a similar fashion to Eq. (10), that is:

$$f_l = 0,079 \left[ \frac{G(1-x)d_i}{\mu_l} \right]^{-0,25} \quad (16)$$

Several methods are presented in the literature to determine the two-phase multiplier and the void fraction, most of them of empirical nature. Carey (1992) presents the correlations developed by Lockhart and Martinelli for these quantities:

$$\phi_l = \left( 1 + \frac{C}{X} + \frac{1}{X^2} \right)^{1/2} \quad (17)$$

$$\alpha = (1 + 0,28 X^{0,71})^{-1} \quad (18)$$

where:

$$X^2 = \frac{\left( \frac{dP}{dz} \right)_l}{\left( \frac{dP}{dz} \right)_v} \quad (19)$$

This quantity is called the Martinelli Parameter, which is the ratio between the pressure drop that would occur if only the liquid phase was present and the pressure drop that would occur if only the vapor phase was present. These two pressure drops are evaluated using equations for single phase flow:

$$\left( \frac{dP}{dz} \right)_l = - \frac{2f_l G^2 (1-x)^2}{\rho_l d_i} \quad (20)$$

$$\left( \frac{dP}{dz} \right)_v = - \frac{2f_v G^2 x^2}{\rho_v d_i} \quad (21)$$

The constant  $C$  which appears in Eq. (17) depends on the nature of the flows:

- $C=20$  for turbulent liquid and vapor flow
- $C=12$  for turbulent vapor and laminar liquid flow
- $C=10$  for laminar vapor and turbulent liquid flow
- $C=5$  for laminar liquid and vapor flow

Carey (1992) present other models for the two-phase multiplier. Wallis (1969) proposes a model where liquid and vapor flow in separated tubes with distinct diameters, but with the same total area as the actual tube. Furthermore, the pressure drops of the two flows must be equal to the pressure drop of the actual flow. For turbulent flow, it yields:

$$\phi_l = \left[ 1 + \left( \frac{1}{X} \right)^{\frac{16}{19}} \right]^{\frac{19}{16}} \quad (22)$$

Finally, the friction coefficient for the liquid phase is calculated with Eq. (16) while the friction coefficient for the vapor phase is calculated with:

$$f_v = 0,079 \left[ \frac{Gx d_i}{\mu_v} \right]^{-0,25} \quad (23)$$

Similarly to the homogenous model, the total length of the condenser is divided in 100 parts and the total pressure drop is calculated numerically as the summation of the pressure drops of the 100 parts. Within each part the quantities given by Eqs. (13) and (15) to (23).

### 3. EXPERIMENTAL STUDY

#### 3.1. Experimental Set-Up

A stainless steel-water loop thermosyphon prototype was built and tested for the heat transfer limit due to pressure drop. The condenser is a stainless-steel 6 mm internal diameter and 11 m horizontal tube with several “U” bends. Figure 4 shows a schematic of the experimental set-up. The prototype maximum allowable hydraulic head (Fig. 2) is  $h_{max}=2$  m. The evaporator is a horizontal cylinder with cartridge heaters immersed in the liquid pool. The heat transfer is computed as the electric power input to the heaters minus the thermal insulation losses.

The condenser is inserted in a controlled thermal bath with (ethylene-glycol) in the forced convection. The temperature of the thermal fluid is controlled through a LAUDA® PR855 controlled temperature thermal bath.

The evaporator of the model is made of a SS 316 horizontal tube with 100 mm i.d. and 400 mm long. The working fluid is distilled water and the filling ratio is 80% of the evaporator volume. The vapor line is connected to the top of the horizontal cylinder, while the liquid return line is connected to the side of the cylinder, below the liquid pool level. Heat is provided by eight 20 mm o.d. cartridge type electrical heaters immersed in the liquid pool. The entire system is insulated with glass wool, with the thermal losses estimated in 100 W. By measuring the electrical resistance and the current, the heat power input could be accurately assessed.

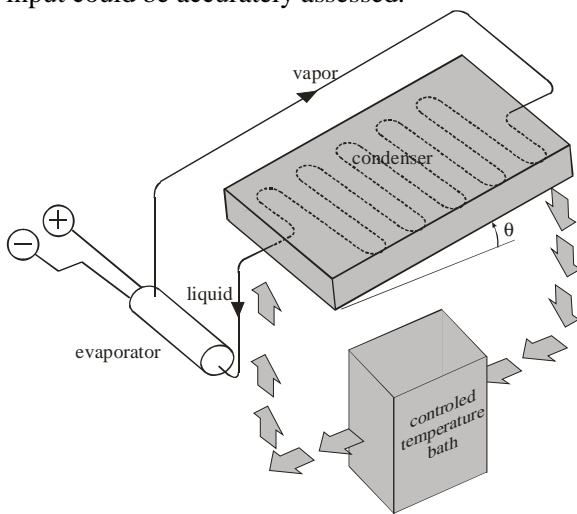


Figure 4. Experimental set-up.

The condenser could also be tilted with respect to the horizontal position (see tilt angle  $\theta$  in Fig. 4). However, preliminary measurements showed the system is not greatly affected by this angle. This is because most part of the condenser remains in horizontal orientation, regardless of the tilt angle. Only the “U” bends experience change in the orientation as the tilt angle is varied. All the tests presented here are for  $\theta=13^\circ$ .

The condenser was instrumented with seven K-type thermocouples distributed evenly over its length. The first thermocouple was placed 50 mm from the start of the condenser. The seventh thermocouple was placed 50 mm from the end of the condenser. Figure 5 present the thermocouple distribution. The vapor line was instrumented with one K-type thermocouple next to the evaporator exit. The evaporator was instrumented with two K-type thermocouples: one immersed in the liquid pool and one immersed in the vapor space above the liquid pool. The controlled thermal bath was measured by two K-type thermocouples, one at the inlet and one at the outlet. The temperature, voltage and current were measured with a HP 3947-A® Data Acquisition System connected to a personal computer, which stored the data for further treatment.

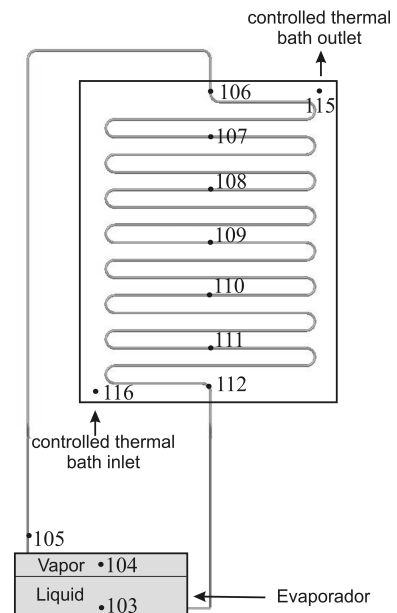


Figure 5. Thermocouple distribution.

### 3.2. Tests Procedure

The heater was turned on starting from the thermal equilibrium with the ambient. The power input was first set to 1000 W. After the system reached steady state, the power input was increased by steps of 500 W. In each power step, the system was left to reach steady state. Before the system reached the heat transfer limit due to pressure drop, the condenser thermocouples give virtually the same reading, which is above the controlled thermal bath, showing the vapor reached the condenser entire length and it is transferring heat to the thermal bath. After the system exceeded the limit, the condensate level floods part of the condenser (Fig. 4). This can be easily noticed by inspecting the thermocouple readings, which give the same readings as the thermocouples of the thermal bath. In this case, that part of the condenser is inactive for heat transfer. At this point, the test was finished and the heater was turned off.

This procedure was repeated for several mean temperature levels of the thermosyphon. The mean temperature level was varied by changing the temperature level of the controlled thermal bath.

### 3.3. Experimental Uncertainty

After calibration of the system, the uncertainty in temperature measurement is  $\pm 0.60^\circ\text{C}$  in the range of temperatures of interest. The uncertainty in voltage measurement is  $\pm 0.1\%$ , and the uncertainty of the heater electrical resistance value was found to be  $\pm 4\%$ .

## 4. RESULTS AND DISCUSSION

Figure 6 presents a comparison between the measured data and the theoretical prediction for the heat transfer limit due to pressure drop. As one can see, different curves are presented. The curves labeled as Cicchitti and McAdams employ the homogenous model with the equivalent viscosity computed through Eqs. (11) and (12), respectively. The curves labeled as Lockhart Martinelli ( $C=12$ ) and Wallis employ the separated model with the two-phase multiplier computed through Eqs. (17) and (22), respectively.

The increase of heat transfer limit with temperature is both predicted theoretically and observed experimentally. The increase is due to changes of thermodynamic properties and also the friction coefficient, which varies with mass flow rate.

The separated model with the two-phase multiplier computed using Wallis' model yielded the best agreement with the measured data. The other models/correlations predicted lower values for the heat transfer limit due to pressure drop.

In order to understand how the authors knew whether the thermosyphon reached the heat transfer limit or not, let's examine Fig. 7. It presents the temperature readings as a function of time for the controlled thermal bath set at  $150^\circ\text{C}$ . As one can see, the evaporator temperatures (103 and 104, Fig. 5) are very close together and approximately  $20^\circ\text{C}$  above the condenser temperatures (106 to 112). The condenser temperature readings also relatively close to each other, with the maximum temperature difference of approximately  $4^\circ\text{C}$ . The difference of temperature readings between the first (106) and the last (112) condenser temperature is less than  $0.8^\circ\text{C}$ , which shows that the condenser cooling is approximately isothermal. For  $\text{time} < 105$  min, the heat transfer rate was  $q=3.9$  kW. At  $\text{time} \approx 105$  min, the system was almost in steady state and the heat transfer rate was suddenly increased to  $q=4.4$  kW. As one can see, the temperature readings experiment a steep increase right after that. The rate of temperature increase with time is approximately the same for all the thermocouples. As the temperature levels rise, they approach steady state again. However, the reading of thermocouple 112 suddenly starts to decrease at  $\text{time} \approx 108$  min, while the others continue increasing.

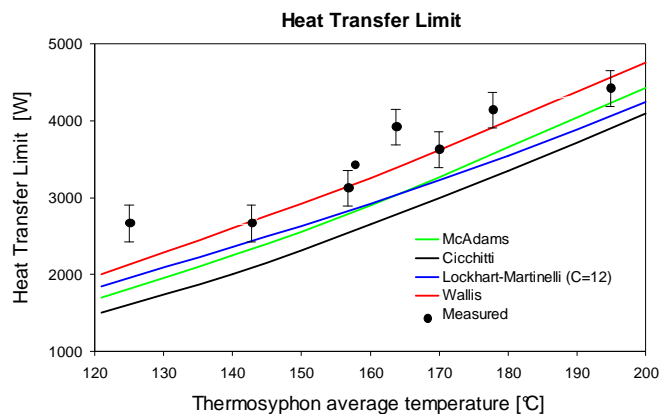


Figure 6. Comparison between theory and data for the heat transfer limit due to pressure drop.

At this very point, the condensate return level reached the thermocouple placed at the end of the

condenser (112), which means the system exceeded the heat transfer limit due to pressure drop. Therefore one concludes that the limit lies between heat transfer rates of 3.9 kW and 4.4 kW. The measured heat transfer limit is defined here as the average of the two values, i.e., approximately 3.15kW. The limit was reached when the thermosyphon mean temperature was 178°C (average of the thermocouple readings from 103 to 112).

All the data points presented in the graph of Fig. 6 were obtained using the procedure described above. The uncertainty of this procedure is 500W, which is the test power step. The amplitude of the error bar is therefore 500W. The error bar then indicates that the limit could be actually anywhere within that range.

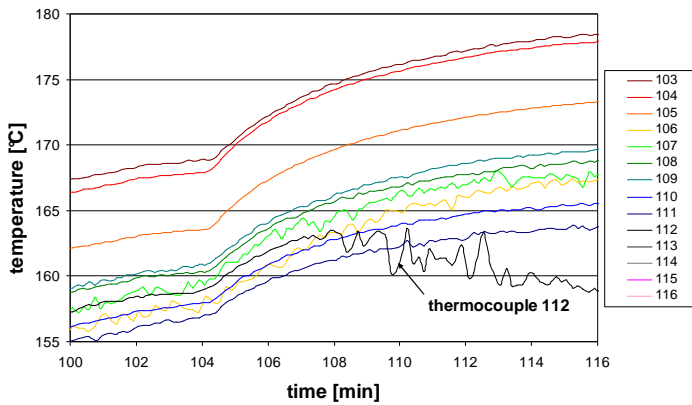


Figure 7. Temperature reading as a function of time.

## 5. CONCLUSIONS

This work presented theoretical and experimental studies on the heat transfer limit due to pressure drop of loop thermosyphons. This limit is specially important for large pressure drops systems, such as heating systems where the condenser is a long steam coil. When the thermosyphon exceeds this limit, the condensate blocks part of the condenser, increasing the overall thermal resistance.

A model is proposed here, which is based on literature models and correlations for pressure drop in both single and two-phase flows. A prototype was built and tested for the heat transfer limit due to pressure drop. The data is relatively well predicted by the proposed model. The model can then be employed as a loop thermosyphon design tool, so the thermosyphon can operate safely below this limit.

## NOMENCLATURE

$A$	cross sectional area [ $m^2$ ]
$C$	constant (see Eq. 18)
$d_i$	inner diameter [m]
$f$	friction coefficient [ ]
$G$	mass flux [ $kg/s.m^2$ ]
$h$	hydraulic head
$h_{lv}$	latent heat of vaporization [J/kg]
$L$	length [m]
$\dot{m}$	mass flow rate [kg/s]
$P$	thermodynamic pressure [Pa]
$q$	heat transfer rate [W]
Re	Reynolds number
$v$	specific volume ( $=1/\rho$ ) [ $m^3/kg$ ]
$V$	velocity [m/s]
$x$	vapor quality [ ]
$X^2$	Martinelli Parameter
$z$	coordinate axis along the flow [m]

### Subscripts

$evap$	evaporator
$cond$	condenser
$e$	equivalent
$l$	liquid
$v$	vapor
$TP$	two-phase

### Greek letters

$\alpha$	void fraction ( $= A_v/A$ ) [ ]
$\phi_l$	two-phase multiplier [ ]
$\mu$	absolute viscosity [Pa.s]
$\rho$	density [ $kg/m^3$ ]
$\Omega$	tube tilt angle [ $^\circ$ ]

## ACKNOWLEDGEMENT

The authors would like to acknowledge the support of PETROBRAS, the Brazilian Petroleum Company, during this research.

## REFERENCES

1. Fox, R. W. & McDonald, A. T., Introdução à Mecânica dos Fluidos, Guanabara Koogan, 3<sup>a</sup>. Edição, Rio de Janeiro, 1988.
2. Collier, J. G. and Thome, J. R., Convective Boiling and Condensation, Clarendon Press, 3<sup>rd</sup> Edition, Oxford, 1994.
3. Wallis, G. B., One-dimensional Two-phase Flow, McGraw-Hill, 1969.
4. Carey, V. P., Liquid-Vapor Phase-Change Phenomena, Taylor & Francis, 1992.